

CHAPTER 1 - INTRODUCTION AND THEORY OF THE COTTON-MOUTON EFFECT

1.1 INTRODUCTION

The phenomenon of magnetic field-induced birefringence, first observed by Kerr,¹ and subsequently by Cotton and Mouton² after whom the effect was named, has been a particularly valuable source of information concerning electric and magnetic properties of molecules. When a magnetic induction is applied to a medium, a birefringence is induced, and the effect has a quadratic dependence on the magnetic induction. The molar Cotton-Mouton constant³ is defined as

$${}_{\text{m}}C = \frac{2nV_{\text{m}}\mu^2}{3(n^2 + 2)^2} \left[\frac{n_{\parallel} - n_{\perp}}{B^2} \right]_{B=0} \quad (1.1)$$

in which n is the mean refractive index, μ is the magnetic permeability, $n_{\parallel} - n_{\perp}$ is the refractive index difference induced in the gas by the magnetic induction, B , and V_{m} is the molar volume. Due to molecular interactions, the molar Cotton-Mouton constant for a gas can be expected to be density dependent; such behaviour is expressed by the virial expansion

$$= A_{\text{C}} + B_{\text{C}}V_{\text{m}}^{-1} + C_{\text{C}}V_{\text{m}}^{-2} + \dots \quad (1.2)$$

where A_{C} and B_{C} are the Cotton-Mouton first and second virial coefficients, respectively. A_{C} represents the molar Cotton-Mouton constant for a gas at low density where molecular interactions are negligible, whereas B_{C} accounts for the contribution of interacting pairs of molecules to ${}_{\text{m}}C$.

1.2 THEORIES OF THE COTTON-MOUTON EFFECT

1.2.1 Classical Statistical Mechanical Theories

Originally developed for the interpretation of the Kerr effect, the classical Langevin-Born theory⁴ has been modified to account for the Cotton-Mouton effect, commonly regarded as the magnetic analogue of the Kerr effect. This theory assumed that the birefringent medium could be regarded as an ideal gas and that the only contribution to the magnetic birefringence arises from partial molecular orientation. Further developments⁵ attempted to account for molecular interactions but fundamental limitations remained owing to the inherent assumptions in the models.

Buckingham and Pople⁶ derived a classical statistical mechanical theory which took account of the dependence of the total molecular polarizability on an applied magnetic field. The radiation field and molecular rotation, vibration and translation were treated classically. In addition, dispersion effects were neglected as the theory considered the static electric polarizability of a molecule in a magnetic field. This assumption should be adequate if the frequency of the optical field is sufficiently remote from an absorption region. An expression for the low-density Cotton-Mouton constant was derived, using the following expansion for the energy, W , of a molecule in a configuration τ (describing the position and orientation of the molecule) in the presence of an electric field, E_α , and magnetic induction, B_α :

$$W(\tau, E_\alpha, B_\alpha) = W^{(0)} - \mu_\alpha^{(0)} E_\alpha - \frac{1}{2} \alpha_{\alpha\beta} E_\alpha E_\beta - \frac{1}{2} \chi_{\alpha\beta} B_\alpha B_\beta - \frac{1}{2} \Omega_{\alpha:\beta\gamma} E_\alpha B_\beta B_\gamma - \frac{1}{4} \eta_{\alpha\beta:\gamma\delta} E_\alpha E_\beta B_\gamma B_\delta - \dots \quad (1.3)$$

where $W^{(0)}$ is the energy in the absence of applied electric or magnetic fields, $\mu_\alpha^{(0)}$ is the permanent electric dipole moment, $\alpha_{\alpha\beta}$ is the electric polarizability, $\chi_{\alpha\beta}$ is the

magnetizability and $\Omega_{\alpha:\beta\gamma}$ and $\eta_{\alpha\beta:\gamma\delta}$ are higher-order tensors. Hence, the polarizability in the presence of a magnetic field is

$$\Pi_{\alpha\beta} = -\frac{\partial^2 W}{\partial E_\alpha \partial E_\beta} = \alpha_{\alpha\beta} + \frac{1}{2} \eta_{\alpha\beta:\gamma\delta} B_\gamma B_\delta + \dots \quad (1.4)$$

Considering the difference $\Pi_{\parallel} - \Pi_{\perp}$ for each configuration and expanding the result as a power series in B_α , it can be shown that the leading non-zero term is in B^2 , hence the definition of ${}_m C$ can be written in the limit of zero density as

$$A_C = \frac{N_A \mu_0^2}{54 \epsilon_0} \left[\frac{\partial^2 \bar{\Pi}}{\partial B^2} \right]_{B=0} \quad (1.5)$$

where N_A is the Avogadro constant, μ_0 is the vacuum permeability, ϵ_0 is the vacuum permittivity, and $\bar{\Pi}$ is a statistical average of the scalar Π . By performing a Boltzmann average over configurations τ on the second derivative in equation (1.5), it can be shown⁶ that

$$A_C = \frac{N_A \mu_0^2}{270 \epsilon_0} \left[\left(\eta_{\alpha\beta:\alpha\beta} - \frac{1}{3} \eta_{\alpha\alpha:\beta\beta} \right) + \frac{\alpha_{\alpha\beta} \chi_{\alpha\beta} - 3\alpha\chi}{kT} \right] \quad (1.6)$$

where $\alpha = \frac{1}{3} \alpha_{\beta\beta}$ is the mean electric polarizability, $\chi = \frac{1}{3} \chi_{\beta\beta}$ is the mean magnetizability (or magnetic susceptibility) and T is the absolute temperature. The first two terms, which are temperature-independent, arise from molecular anisotropy induced directly by the applied magnetic field and are the only contributions to A_C for molecules whose polarizability and magnetizability tensors are isotropic and for quasispherical molecules. The temperature-dependent term is equivalent to the Langevin-Born expression for a diamagnetic molecule and is non-zero whenever $\alpha_{\alpha\beta}$ and $\chi_{\alpha\beta}$ are anisotropic. For molecules with an axis of three-fold or higher symmetry, equation (1.6) simplifies to

$$A_C = \frac{N_A \mu_0^2}{270 \epsilon_0} \left[\left(\eta_{\alpha\beta:\alpha\beta} - \frac{1}{3} \eta_{\alpha\alpha:\beta\beta} \right) + \frac{2\Delta\alpha\Delta\chi}{3kT} \right] \quad (1.7)$$

where $\Delta\alpha = \alpha_{zz} - \alpha_{xx}$ is the optical-frequency polarizability anisotropy and $\Delta\chi = \chi_{zz} - \chi_{xx}$ is the magnetizability (or magnetic) anisotropy (z is coincident with the symmetry axis and x is orthogonal to z).

Buckingham and Pople⁶ also showed that, for axially symmetric molecules, ${}_mC$ should be independent of density if intermolecular angular correlations are absent. By considering the contribution to the Cotton-Mouton constant involving two-body interactions between centrosymmetric molecules, an expression⁶⁻⁸ was obtained for B_C . Evaluation of B_C for some typical molecules in this class indicates that such contributions to ${}_mC$ should be small at normal temperatures and pressures.

1.2.2 Quantum Mechanical Theories

Classically, it is assumed that a molecule can possess a continuous range of configurations, thus a quantum mechanical description of the Cotton-Mouton effect requires the evaluation of

$$\langle \Pi_{\parallel} - \Pi_{\perp} \rangle = \frac{\sum_j \langle U_j | \Pi_{\parallel} - \Pi_{\perp} | U_j \rangle \exp(-W_j^{(0)}/kT)}{\sum_j \exp(-W_j^{(0)}/kT)} \quad (1.8)$$

for the states $|U_j\rangle$ of a system. If the optical field is treated classically, and molecular rotation and vibration quantum mechanically, it can be shown^{8,9} that for a linear closed-shell diamagnetic molecule in its ground vibrational state,

$$A_C = \frac{N_A \mu_0^2}{270 \epsilon_0} \left[\left(\eta_{\alpha\beta:\alpha\beta} - \frac{1}{3} \eta_{\alpha\alpha:\beta\beta} \right) + \frac{2\Delta\alpha\Delta\chi}{3kT} \left(1 - \sigma_0 + \frac{8}{15} \sigma_0^2 - \dots \right) \right] \quad (1.9)$$

where $\sigma_0 = \frac{hcB_0}{kT}$ and B_0 is the rotational constant in the ground vibrational state. The evaluation of the term $\left(1 - \sigma_0 + \frac{8}{15} \sigma_0^2 - \dots \right)$ at 300 K for various molecules (for example H₂, 0.76; N₂, 0.99) indicates that, at such temperatures, rotational quantum corrections are significant only for molecules with large rotational constants, such as hydrogen and diatomic hydrides.

Kling, Dreier and Hüttner¹⁰ derived an expression for the Cotton-Mouton constant of a paramagnetic gas by treating molecular rotation and vibration quantum mechanically. Their expression for A_C is too lengthy to reproduce here but it can be shown that, for a diamagnetic molecule at about 300 K, quantum corrections are negligible for all but the lightest molecules. In addition, contributions from rotationally induced magnetic moments may be neglected.

A quantum electrodynamic theory has been developed by Atkins, Barron and Miller^{11,12} for a range of important optical phenomena. The theory incorporates a formalism in which the physical processes involved are described using the S - and R -matrix method, and the polarizations of incident and emergent light by the Stokes parameters which can be evaluated as the expectation values of the Stokes operators. The assumption of classical molecular motion in the derivation given by Atkins and Miller¹² can be removed by the inclusion of quantized rotation and vibration. Their theory provides formal justification for the assumption, made in other theories of magnetic birefringence, that the radiation field can be treated classically in respect of this effect.

1.3 SOME RELEVANT ELECTRIC AND MAGNETIC PROPERTIES

As previously mentioned, the determination of the molar Cotton-Mouton constant over a range of temperatures allows the evaluation of various important electric and magnetic properties which will be briefly discussed in this section.

1.3.1 The Electric Polarizability

The electric dipole polarizability, $\alpha_{\alpha\beta}$, also known as the first order polarizability, describes the electric dipole moment induced in a molecule by an electric field. From equation (1.4), it can be seen that, for static polarizabilities,

$$\alpha_{\alpha\beta} = - \left(\frac{\partial^2 W}{\partial E_\alpha \partial E_\beta} \right)_{E=B=0} \quad (1.10)$$

Quantum-mechanical perturbation theory predicts that, for optical frequencies ω well removed from the transition frequencies ω_{kn} , the polarizability of a molecule in the n th non-degenerate state is given by:^{13,14}

$$\alpha_{\alpha\beta}^{(n)}(-\omega; \omega) = \sum_k \frac{2\omega_{kn}}{\hbar(\omega_{kn}^2 - \omega^2)} \langle n | \mu_\alpha | k \rangle \langle k | \mu_\beta | n \rangle \quad (1.11)$$

where μ_α is the electric dipole moment operator, n and k are electronic and vibrational, but not rotational, states.

To determine magnetizability anisotropies, $\Delta\chi$, from studies of the temperature-dependence of the Cotton-Mouton effect, it is necessary to have accurate values of optical-frequency polarizability anisotropies. The most important source of such data is the depolarization ratio, ρ_0 , for Rayleigh scattered light.^{15,16} In the

absence of magnetic fields, the depolarization of Rayleigh scattered light is determined by the polarizability anisotropy parameter

$$\kappa^2 = \frac{3\alpha_{\alpha\beta}\alpha_{\alpha\beta} - \alpha_{\alpha\alpha}\alpha_{\beta\beta}}{2\alpha_{\alpha\alpha}\alpha_{\beta\beta}} \quad (1.12)$$

For linearly polarized incident light, the depolarization ratio is related to the polarizability anisotropy parameter by the classical expression¹⁵

$$\rho_0 = \frac{3\kappa^2}{5 + 4\kappa^2} \quad (1.13)$$

The equation above is valid for all but the lightest molecules provided both the rotational Raman spectrum and the Rayleigh line are included in the measurement, while the vibrational Raman lines are excluded.¹⁵ There are various assumptions in the classically derived theory but quantum effects have been shown¹⁵ to be negligible for most molecules. For H₂, inclusion of rotational quantum corrections¹⁵ reduces the depolarization ratio measured at 632.8 nm to 91% of the classical value. Of more importance, spurious contributions from depolarized Raman scattering can lead to significant overestimation of the depolarization ratio and, thus, of the derived polarizability anisotropy. For molecules that have a weakly anisotropic polarizability, the vibrational Raman scattering may be removed with a monochromator or filter of sufficient bandwidth to ensure inclusion of all rotational Raman lines in the observed scattering intensity. This difficulty can also be avoided by evaluating the intensity of perpendicularly polarized light relative to the incident beam using features in the rotational Raman spectrum.¹⁷ For molecules with an axis of three-fold or higher symmetry, equation (1.12) simplifies to

$$\kappa = \frac{\Delta\alpha}{3\alpha} \quad (1.14)$$

The mean optical-frequency polarizability, α , is conveniently determined from measurements of the refractive index.¹⁴ Measurement of the dielectric constant¹⁴ provides the mean static polarizability, α^0 . Static polarizability anisotropies of dipolar molecules can be obtained from the second order Stark effect^{14,18} whereas Stark shifts from molecular beam techniques¹⁹ provide such values for nondipolar molecules.

For molecules with three different principal polarizabilities, the relative intensities in the Raman spectrum depend on the irreducible spherical tensor components α_0^2 and $\alpha_2^2 + \alpha_{-2}^2$ of the polarizability.²⁰ Comparison of observed and calculated rotational Raman spectra allows the evaluation of the ratio

$$R_{20} = \frac{\alpha_2^2 + \alpha_{-2}^2}{\alpha_0^2} \quad (1.15)$$

For molecules of C_{2v} or higher symmetry, equation (1.15) becomes, in terms of Cartesian tensor components of the polarizability,

$$R_{20} = \frac{\sqrt{6}(\alpha_{xx} - \alpha_{yy})}{2\alpha_{zz} - \alpha_{xx} - \alpha_{yy}} \quad (1.16)$$

in which a prolate-top Cartesian axis system has been chosen, that is, where the z axis is identified with the smallest moment of inertia of the molecule, and the y axis is with the largest moment of inertia.

In conjunction with values of the mean polarizability and the depolarization ratio, a value of R_{20} can be used in the derivation of components of the polarizabilities for a molecule.

Measurements of the electrooptical Kerr effect in gases and vapours provide information about the molecular polarizability and other molecular properties.^{14,21} The effect results from the birefringence induced in a medium by a uniform electric field, and has a quadratic dependence on the electric field strength. The molar Kerr constant is defined as²²

$$\begin{aligned} {}_mK &= \frac{6nV_m}{(n^2 + 2)^2(\epsilon_r + 2)^2} \left[\frac{n_{\parallel} - n_{\perp}}{E^2} \right]_{E=0} \\ &= A_K + B_K V_m^{-1} + C_K V_m^{-2} + \dots \end{aligned} \quad (1.17)$$

where ϵ_r is the relative permittivity of the medium and A_K , B_K , C_K are the Kerr virial coefficients. From the classical mechanical treatment by Buckingham and Pople,²² the Kerr first virial coefficient, A_K , is related to molecular properties by

$$\begin{aligned} A_K &= \frac{N_A}{81\epsilon_0} \left\{ \gamma^K + \frac{1}{kT} \left[\frac{2}{3} \mu \beta^K + \frac{3}{10} (\alpha_{\alpha\beta}^0 \alpha_{\alpha\beta}^0 - 3\alpha\alpha^0) \right] \right. \\ &\quad \left. + \frac{3}{10} \frac{1}{(kT)^2} \mu^2 (\alpha_{zz} - \alpha) \right\} \end{aligned} \quad (1.18)$$

in which μ is the permanent electric dipole moment whose direction defines the z -axis, $\alpha_{\alpha\beta}^0$ is the static polarizability tensor, and β^K and γ^K are the mean first and second Kerr hyperpolarizabilities, respectively. For nondipolar molecules with an axis of three-fold or higher symmetry, equation (1.18) simplifies to

$$A_K = \frac{N_A}{405\epsilon_0} \left[5\gamma^K + (kT)^{-1} \Delta\alpha\Delta\alpha^0 \right] \quad (1.19)$$

where $\Delta\alpha^0$ is the static polarizability anisotropy. Measurements^{14,21} of the temperature dependence of A_K have led to values of γ^K and $\Delta\alpha^0$ for axially-

symmetric nondipolar molecules, and β^K and $\alpha_{zz} - \alpha$ for dipolar species. The Kerr effect of liquids and dilute solutions²³ provides values of molecular properties that are not directly descriptive of free molecules, due to complications arising from molecular interactions and local-field effects.

1.3.2 The Magnetizability

As with the polarizability tensor in equation (1.10), the magnetizability tensor²⁴

$$\chi_{\alpha\beta} = - \left(\frac{\partial^2 W}{\partial B_\alpha \partial B_\beta} \right)_{E=B=0} \quad (1.20)$$

can be defined in terms of the magnetic induction, B . From perturbation theory,²⁴⁻²⁶ the magnetizability, also known as the magnetic susceptibility, of a diamagnetic molecule can be expressed as a sum of diamagnetic and temperature-independent paramagnetic terms:

$$\begin{aligned} \chi_{\alpha\beta} = & -\frac{e^2}{4m_e} \langle 0 | \sum_i [r_i^2 \delta_{\alpha\beta} - r_{i\alpha} r_{i\beta}] | 0 \rangle \\ & + \frac{e^2 \hbar^2}{4m_e^2} \sum_{k \neq 0} \frac{\langle 0 | \hat{L}_\alpha | k \rangle \langle k | \hat{L}_\beta | 0 \rangle + \langle 0 | \hat{L}_\beta | k \rangle \langle k | \hat{L}_\alpha | 0 \rangle}{W_k - W_0} = \chi_{\alpha\beta}^d + \chi_{\alpha\beta}^p \end{aligned} \quad (1.21)$$

where $r_{i\alpha}$ is the position vector for the i th electron, \hat{L}_α is the total electronic orbital angular momentum operator, W_k is the energy of the k th state in the absence of an applied field, and e and m_e are the charge and the mass of an electron, respectively.

The theoretical and experimental aspects of the magnetizability have been extensively examined²⁵⁻³⁰ and the property is of considerable importance in a wide

range of phenomena, such as in studies of the charge distributions in molecules, in nuclear magnetic resonance spectroscopy, in models of the magnetic properties of “aromatic” systems, and in the development of simple bond additivity systems. Several techniques, including oriented-crystal measurements, NMR shieldings and line splittings, molecular beam experiments, beam-maser and conventional microwave Zeeman spectroscopy and the Cotton-Mouton effect, have been employed to obtain experimental information concerning the magnetizability tensor. Of these techniques, the Zeeman effect has been the most widely used; however, this effect is not observable for nondipolar molecules and, consequently, the Cotton-Mouton effect is particularly useful for the study of such species.

The molecular quadrupole moment, Θ , for molecules possessing an axis of three-fold or higher symmetry (z -axis) can be described by the following expression:

$$\Theta = e \sum_n Z_n (z_n^2 - x_n^2) - e \langle 0 | \sum_i (z_i^2 - x_i^2) | 0 \rangle \quad (1.22)$$

where Z_n is the atomic number of the n th nucleus. From equation (1.21), the magnetic anisotropy, $\Delta\chi$, of an axially symmetric molecule can be expressed as

$$\Delta\chi = \Delta\chi^d + \Delta\chi^p \quad (1.23)$$

It is easily shown that equations (1.21), (1.22) and (1.23) allow the separation of $\Delta\chi$ into oppositely-signed diamagnetic and temperature-independent paramagnetic contributions. In addition, the elements of the molecular rotational g tensor, $g_{\alpha\beta}$, the magnetizability anisotropy and the quadrupole moment are related; for a rigid axially symmetric molecule, the following equation applies

$$g_{zz}I_{zz} - g_{xx}I_{xx} = -\left(\frac{m_p}{e}\right) \left[\left(\frac{4m_e}{e}\right) \Delta\chi + \Theta \right] \quad (1.24)$$

where $I_{\alpha\beta}$ is the moment of inertia and m_p is the mass of the proton. If the molecule is planar, the above equation simplifies further to

$$g_{zz} - \frac{1}{2}g_{xx} = -\left(\frac{m_p}{eI_{zz}}\right)\left[\left(\frac{4m_e}{e}\right)\Delta\chi + \Theta\right] \quad (1.25)$$

and if the molecule is linear to

$$g = \left(\frac{m_p}{eI}\right)\left[\left(\frac{4m_e}{e}\right)\Delta\chi + \Theta\right] \quad (1.26)$$

assuming in each case that the molecule is rigid. The effect of molecular vibrations on the validity of equations (1.24) - (1.26) is somewhat difficult to quantify as it may differ for each molecule; however, from a study of hydrogen isotopomers,²⁴ it was concluded that the correction is likely to be insignificant.

Individual values of g_{zz} and g_{xx} cannot be determined from equations (1.24) or (1.25), but it is of interest to use the values of $\Delta\chi$ and Θ , from birefringence experiments, to evaluate the right-hand side of the above equations, which can alternatively be estimated from reported g values and the known molecular structures. It is obvious from equation (1.26) that a single value of g can be obtained if values of $\Delta\chi$ and Θ are known.

1.3.3 The Second Magnetic Hyperpolarizability

This fourth order tensor⁶ can be defined as

$$\eta_{\alpha\beta:\gamma\delta} = -\left(\frac{\partial^4 W}{\partial E_\alpha \partial E_\beta \partial B_\gamma \partial B_\delta}\right)_{E=B=0} \quad (1.27)$$

and is symmetric in the separate pairs (α, β) and (γ, δ) of suffixes. Of its 81 elements, up to 36 may be independent. The property may be considered to describe the quadratic dependence of the molecular polarizability on a magnetic field, as in equation (1.4), or, alternatively, the dependence of the molecular magnetizability on an electric field as described in the following expression:

$$X_{\alpha\beta} = \chi_{\alpha\beta} + \frac{1}{2} \eta_{\gamma\delta:\alpha\beta} E_{\gamma} E_{\delta} + \dots \quad (1.28)$$

where $X_{\alpha\beta}$ represents the magnetizability in the presence of an electric field.

As with $\chi_{\alpha\beta}$, $\eta_{\alpha\beta:\gamma\delta}$ can be partitioned into diamagnetic, temperature-independent paramagnetic and, for the case of paramagnetic molecules, temperature-dependent paramagnetic contributions, as in the relation below:

$$\eta_{\alpha\beta:\gamma\delta} = \eta_{\alpha\beta:\gamma\delta}^d + \eta_{\alpha\beta:\gamma\delta}^p \quad (1.29)$$

For species with spherical symmetry, $\eta_{\alpha\beta:\gamma\delta}$ simplifies to an isotropic tensor of order four, described by:

$$\eta_{\alpha\beta:\gamma\delta} = \eta_{zz:xx} \delta_{\alpha\beta} \delta_{\gamma\delta} + \frac{1}{2} (\eta_{zz:zz} - \eta_{zz:xx}) (\delta_{\alpha\gamma} \delta_{\beta\delta} + \delta_{\alpha\delta} \delta_{\beta\gamma}) \quad (1.30)$$

Using second-order perturbation theory, Buckingham and Pople³¹ calculated the diamagnetic and paramagnetic components of $\eta_{\alpha\beta:\gamma\delta}$ for the hydrogen atom, while neglecting the effect of electron spin. Taking the origin of the axis system as the centre of the atom with spherical symmetry in the absence of an electric field, no paramagnetic contribution is induced parallel to the field, thus $\eta_{zz:zz}^p = 0$. Nevertheless, there is a paramagnetic contribution in a direction orthogonal to the applied electric field. It was deduced that the relatively large electronic transition

energies, $W_k - W_0$, for the hydrogen atom lead to a small orthogonal paramagnetic contribution, $\eta_{zz:xx}^P$, therefore $\Delta\eta$ is dominated by diamagnetic terms. For molecules which distort relatively easily and for those with small electronic transition energies, $\eta_{zz:xx}^P$ may increase, leading to negative values of A_C . It should be noted that while the sign of the temperature-independent term, $\eta_{\alpha\beta:\alpha\beta} - \frac{1}{3}\eta_{\alpha\alpha:\beta\beta}$, is determined by the relative contributions of the diamagnetic and paramagnetic hyperpolarizability terms, the temperature-dependent term, $(N_A\mu_0^2/270\varepsilon_0kT)(\alpha_{\alpha\beta}\chi_{\alpha\beta} - 3\alpha\chi)$, will normally predominate in relation to the sign and magnitude of A_C .

Theoretical calculations of magnetic hyperpolarizability anisotropies have appeared,³² though only for simple species such as hydrogen, deuterium, the rare gases and methane.

1.4 DISCUSSION

The most prolific source of magnetizability anisotropies has been the gas-phase microwave spectroscopic method developed by Flygare and his collaborators.^{33,34} However, many species of interest either lack a permanent electric dipole moment or are too large to be studied easily by microwave spectroscopy. The Cotton-Mouton effect has proved to be a useful technique to study a wide variety of molecules that cannot be, in addition to those that can be, examined by the Zeeman effect.

The aim of this study was to determine electric and magnetic properties of isolated, non-interacting molecules, which can be obtained from the vapour-phase Cotton-Mouton effect. As noted above, there are two contributions to the Cotton-Mouton effect: first, a temperature-independent contribution arising from the

distortion of the electronic structure by the magnetic field and second, a temperature-dependent contribution due to molecular orientation by the field. These experimental investigations involve both density and temperature dependence measurements. The density dependence measurements provide the free-molecule Cotton-Mouton constants, A_C , whereas the temperature dependence measurements allow separation of $A_C T^{-1}$ into the temperature-independent hyperpolarizability and temperature-dependent orientational terms. Numerous temperature dependence vapour-phase Cotton-Mouton effect studies have been published,^{10,35-51} mostly for small molecules which exist as gases at room temperature.

Much of the early work in the field of magnetic birefringence was performed on substances as solutes at high dilution, mainly because the observed birefringence is several orders of magnitude larger than that encountered with gases. Analysis of solution-phase Cotton-Mouton constants yields the term $\Delta\alpha\Delta\chi$ and the magnetic hyperpolarizability term is assumed negligible. Such studies have provided much valuable information, particularly in the determination of molecular magnetizability anisotropies from measurements on pure liquids and dilute solutions,^{52,53} apparent polarizabilities of species⁵⁴ and conformational analysis.⁵⁵ Magnetizability anisotropies, in contrast to polarizability anisotropies, are considered to be virtually independent of physical state.⁵³ Gas-phase studies⁵⁶ which consist of a single-temperature measurement have been reported, but any conclusions from these measurements are dependent on the validity of the assumption regarding the magnetic hyperpolarizability contribution.

Prior to the mid-1980's, there was little information concerning $\Delta\eta$ and early Cotton-Mouton effect studies assumed $\Delta\eta = 0$ in the evaluation of molecular magnetizability anisotropies. Such results, even for strongly anisotropic molecules, have been treated with some caution; in fact, it has repeatedly been suggested^{27-30,57}

that their reliability is compromised by the assumption in respect of the temperature-independent contribution. A knowledge of the true values of the properties would provide a test of this assumption and reliable information that would be of interest for comparison with values obtained from theoretical calculations.

The present work continues previous studies³⁹ with the aim of establishing reliable values of the molecular polarizability anisotropy or the molecular magnetizability anisotropy and other fundamental electric and magnetic properties for a range of molecules. Some of these results were complemented by theoretical calculations carried out in this laboratory. Much of the previous work had concentrated on highly anisotropic molecules, which have large Cotton-Mouton constants, and it was of considerable interest to extend the study to weakly anisotropic species, which have small Cotton-Mouton constants. Evidence for weakly anisotropic molecules indicated that the magnetic hyperpolarizability anisotropy contributes significantly to the Cotton-Mouton effect at normal temperatures and that it must be taken into account in order to derive reliable magnetic anisotropies for such molecules. A study of the methyl halides provided a basis for comparison of results obtained from the Cotton-Mouton effect, microwave Zeeman method and NMR techniques. Another similar study, on carbon dioxide, carbonyl sulfide, and carbon disulfide, has enabled another useful comparison to be made with similar studies undertaken elsewhere.

The following chapters describe significant improvements to the apparatus, originally described by Lukins,³⁹ which was used to perform the Cotton-Mouton effect measurements, and present the results and conclusions for the molecules that were studied.

1.5 REFERENCES

1. J. Kerr, *Report Brit. Assoc.*, 568 (1901).
2. A. Cotton and H. Mouton, *C. R. Hebd. Seances Acad. Sci.*, **141**, 317, 349 (1905).
3. G. Otterbein, *Phys. Z.*, **35**, 249 (1934).
4. (a) P. Langevin, *Radium*, **7**, 249 (1910). (b) P. Langevin, *C. R. Hebd. Seances Acad. Sci.*, **151**, 475 (1910). (c) M. Born, *Ann. Phys., Lpz.*, **55**, 177 (1918). (d) M. Born, *Optik* (Springer, Berlin, 1933).
5. (a) C.V. Raman and K.S. Krishnan, *Proc. Roy. Soc. A*, **117**, 1 (1927). (b) A. Piekara, *Phys. Z.*, **108**, 395 (1938). (c) O. Snellman, *Phil. Mag.*, **40**, 983 (1949).
6. A.D. Buckingham and J.A. Pople, *Proc. Phys. Soc. B*, **69**, 1133 (1956).
7. S. Kielich, *Acta Phys. Polon.*, **22**, 65, 299 (1962).
8. M.G. Corfield, *Ph.D. Thesis* (University of Bristol, 1969).
9. A.D. Buckingham and B.J. Orr, *Proc. Roy. Soc. A*, **305**, 259 (1968).
10. H. Kling, E. Dreier and W. Hüttner, *J. Chem. Phys.*, **78**, 4309 (1983).
11. P.W. Atkins and L.D. Barron, *Proc. Roy. Soc. A*, **304**, 303; **306**, 119 (1968).
12. P.W. Atkins and M.H. Miller, *Mol. Phys.*, **15**, 491, 503 (1968).
13. A.D. Buckingham, "Permanent and Induced Molecular Moments and Long-Range Intermolecular Forces", in *Advances in Chemical Physics* (J.O. Hirschfelder editor), Vol. 12, 107 (Interscience, New York, 1967).

14. M.P. Bogaard and B.J. Orr, "Electric Dipole Polarizabilities of Atoms and Molecules", in *MTP International Review of Science, Physical Chemistry, Series 2, Vol. 2* (A.D. Buckingham editor), 149 (Butterworths, London, 1975).
15. N.J. Bridge and A.D. Buckingham, *Proc. Roy. Soc. A*, **295**, 334 (1966).
16. (a) G.R. Alms, A.K. Burnham and W.H. Flygare, *J. Chem. Phys.*, **63**, 3321 (1975). (b) M.P. Bogaard, A.D. Buckingham, R.K. Pierens and A.H. White, *J. Chem. Soc., Faraday Trans. 1*, **74**, 3008 (1978). (c) F. Baas and K.D. Van den Hout, *Physica A*, **95**, 597 (1979). (d) J.E.M. Haverkort, F. Baas and J.J.M. Beenakker, *Chem. Phys.*, **79**, 105 (1983). (e) M.R. Hesling, *Ph.D. Thesis* (University of New England, 1990).
17. (a) W.F. Murphy, *J. Chem. Phys.*, **67**, 5877 (1977). (b) M. Monan, J.-L. Bribes and R. Gaufrès, *J. Raman Spectrosc.*, **12**, 190 (1982).
18. A.D. Buckingham, "The Stark Effect", in *MTP International Review of Science, Physical Chemistry, Series 1* (D.A. Ramsay editor), Vol. 3, 73 (Butterworths, London, 1972).
19. (a) T.R. Dyke and J.S. Muentner, "The Properties of Molecules from Molecular Beam Spectroscopy", in *MTP International Review of Science, Physical Chemistry, Series 2* (A.D. Buckingham editor), Vol. 2, 27 (Butterworths, London, 1975). (b) T.E. Gough, B.J. Orr and G. Scoles, *J. Mol. Spectrosc.*, **99**, 143 (1983). (c) Y-T. Chen and T. Oka, *J. Chem. Phys.*, **88**, 5282 (1988).
20. (a) J.A. Koningstein, *Introduction to the theory of the Raman effect* (D. Reidel, Dordrecht-Holland, 1972). (b) G.W. Hills and W.J. Jones, *J. Chem. Soc., Faraday Trans. 2*, **71**, 812 (1975). (c) W.F. Murphy, *J. Raman Spectrosc.*, **11**, 339 (1981).

21. (a) I.R. Gentle, *Ph.D. Thesis* (University of Sydney, 1987). (b) I.R. Gentle, D.R. Laver and G.L.D. Ritchie, *J. Phys. Chem.*, **93**, 3035 (1989). (c) I.R. Gentle and G.L.D. Ritchie, *J. Phys. Chem.*, **93**, 7740 (1989). (d) I.R. Gentle, M.R. Hesling and G.L.D. Ritchie, *J. Phys. Chem.*, **94**, 1844 (1990). (e) I.R. Gentle, D.R. Laver and G.L.D. Ritchie, *J. Phys. Chem.*, **94**, 3434 (1990).
22. A.D. Buckingham and J.A. Pople, *Proc. Phys. Soc. A*, **68**, 905 (1955).
23. C.G. LeFèvre and R.J.W. LeFèvre, *Techniques of Chemistry* (A. Weissberger editor), Vol. 1, Part 3C, 399 (Wiley, New York, 1972).
24. A.D. Buckingham and J.E. Cordle, *Mol. Phys.*, **28**, 1037 (1974).
25. J.H. Van Vleck, *Electric and Magnetic Susceptibilities* (Oxford University Press, New York, 1932).
26. W.H. Flygare and R.C. Benson, *Mol. Phys.*, **20**, 225 (1971).
27. R. Ditchfield, "Magnetic Susceptibilities of Diamagnetic Molecules", in *MTP International Review of Science, Physical Chemistry, Series 1* (A.D. Buckingham editor), Vol. 2, 91 (Butterworths, London, 1972).
28. B.R. Appleman and B.P. Dailey, "Magnetic Shielding and Susceptibility Anisotropies", in *Advances in Magnetic Resonance* (J.S. Waugh editor), Vol. 7, 231 (Academic Press, New York, 1974).
29. W.H. Flygare, *Chem. Rev.*, **74**, 653 (1974).
30. D.H. Sutter and W.H. Flygare, "The Molecular Zeeman Effect", in *Topics in Current Chemistry*, Vol. 63, 89 (Springer, Heidelberg, 1976).
31. A.D. Buckingham and J.A. Pople, *Proc. Camb. Phil. Soc.*, **53**, 262 (1957).

32. (a) P.W. Fowler and A.D. Buckingham, *Mol. Phys.*, **67**, 681 (1989). (b) D.M. Bishop, S.M. Cybulski and J. Pipin, *J. Chem. Phys.*, **94**, 6686 (1991). (c) M.J. Jamieson, *Chem. Phys. Lett.*, **183**, 9 (1991). (d) D.M. Bishop and J. Pipin, *Chem. Phys. Lett.*, **186**, 195 (1991). (e) M. Jaszuński, H.J.Aa. Jensen, P. Jørgensen, A. Rizzo, T. Helgaker and K. Ruud, *Chem. Phys. Lett.*, **191**, 599 (1992). (f) D.M. Bishop and S.M. Cybulski, *Chem. Phys. Lett.*, **200**, 153 (1992).
33. W. Hüttner and W.H. Flygare, *J. Chem. Phys.*, **47**, 4137 (1967).
34. W. Hüttner, M.-K. Lo, W.H. Flygare, *J. Chem. Phys.*, **48**, 1206 (1968).
35. H. Geschka, S. Pferrer, H. Haüssler and W. Hüttner, *Ber. Bunsenges Phys. Chem.*, **86**, 790 (1982).
36. H. Kling, H. Geschka and W. Hüttner, *Chem. Phys. Lett.*, **96**, 631 (1983).
37. P.B. Lukins, A.D. Buckingham and G.L.D. Ritchie, *J. Phys. Chem.*, **88**, 2414 (1984).
38. H. Kling and W. Hüttner, *Chem. Phys.*, **90**, 207 (1984).
39. P.B. Lukins, *Ph.D. Thesis* (University of Sydney, 1984).
40. P.B. Lukins, D.R. Laver, A.D. Buckingham and G.L.D. Ritchie, *J. Phys. Chem.*, **89**, 1309 (1985).
41. P.B. Lukins and G.L.D. Ritchie, *J. Phys. Chem.*, **89**, 3409 (1985).
42. H. Kling and W. Hüttner, *Mol. Phys.*, **56**, 303 (1985).
43. F. Scuri, G. Stefanini, E. Zavattini, E. Iacopini and E. Polacco, *J. Chem. Phys.*, **85**, 1789 (1986).

44. W. Hüttner, H. Träuble, H.U. Wieland and H. Müller, *Chem. Phys. Lett.*, **140**, 421 (1987).
45. P.B. Lukins and G.L.D. Ritchie, *J. Phys. Chem.*, **92**, 2013 (1988).
46. M.H. Coonan and G.L.D. Ritchie, *J. Phys. Chem.*, **95**, 1220 (1991).
47. P.B. Lukins and G.L.D. Ritchie, *Chem. Phys. Lett.*, **180**, 551 (1991).
48. R. Cameron, G. Cantatore, A.C. Melissinos, J. Rogers, Y. Semertzidis, H. Halama, A. Prodell, F.A. Nezrick, C. Rizzo and E. Zavattini, *J. Opt. Soc. Am. B*, **8**, 520 (1991).
49. R. Cameron, G. Cantatore, A.C. Melissinos, Y. Semertzidis, H. Halama, D. Lazarus, A. Prodell, F.A. Nezrick, P. Micossi, C. Rizzo, G. Ruoso and E. Zavattini, *Phys. Lett. A*, **157**, 125 (1991).
50. M.H. Coonan, I.E. Craven, M.R. Hesling, G.L.D. Ritchie and M.A. Spackman, *J. Phys. Chem.*, **96**, 7301 (1992).
51. M.H. Coonan and G.L.D. Ritchie, *Chem. Phys. Lett.*, **202**, 237 (1993).
52. (a) R.J.W. LeFèvre, P.H. Williams and J.M. Eckert, *Aust. J. Chem.*, **18**, 1133 (1965). (b) R.J.W. LeFèvre and D.S.N. Murthy, *Aust. J. Chem.*, **19**, 179 (1966). (c) R.J.W. LeFèvre, D.S.N. Murthy and P.J. Stiles, *Aust. J. Chem.*, **21**, 3059 (1968). (d) M.R. Battaglia and G.L.D. Ritchie, *Mol. Phys.*, **32**, 1481 (1976). (e) M.R. Battaglia and G.L.D. Ritchie, *J. Chem. Soc., Faraday Trans. 2*, **73**, 209 (1977). (f) M.R. Battaglia, *Chem. Phys. Lett.*, **54**, 124 (1978). (g) P.J. Batchelor, J.V. Champion and G.H. Meeten, *J. Chem. Soc., Faraday Trans. 2*, **76**, 1610 (1980). (h) M.P. Brereton, M.K. Cooper, G.R. Dennis and G.L.D. Ritchie, *Aust. J. Chem.*, **34**, 2253 (1981). (i) G.L.D. Ritchie and J. Vrbancich, *Aust. J. Chem.*, **35**, 869 (1982). (j) E.W. Blanch, G.R. Dennis, G.L.D. Ritchie

- and P. Wormell, *J. Mol. Struct.*, **248**, 201 (1991). (k) J.H. Williams and J. Torbet, *J. Phys. Chem.*, **96**, 10477 (1992).
53. C.L. Cheng, D.S.N. Murthy and G.L.D. Ritchie, *Mol. Phys.*, **22**, 1137 (1971).
54. (a) C.L. Cheng, D.S.N. Murthy and G.L.D. Ritchie, *Aust. J. Chem.*, **25**, 1301 (1972). (b) R.L. Calvert and G.L.D. Ritchie, *J. Chem. Soc., Faraday Trans. 2*, **76**, 1249 (1980). (c) G.R. Dennis, I.R. Gentle and G.L.D. Ritchie, *J. Chem. Soc., Faraday Trans. 2*, **79**, 529 (1983). (d) G.R. Dennis, I.R. Gentle, G.L.D. Ritchie and C.G. Andrieu, *J. Chem. Soc., Faraday Trans. 2*, **79**, 539 (1983).
55. (a) C.L. Cheng, D.S.N. Murthy and G.L.D. Ritchie, *J. Chem. Soc., Faraday Trans. 2*, **68**, 1679 (1972). (b) J. Vrbancich, *Ph.D. Thesis* (University of Sydney, 1979). (c) G.L.D. Ritchie and J. Vrbancich, *J. Mol. Struct.*, **78**, 279 (1982). (d) D. Mirarchi, L. Phillips and G.L.D. Ritchie, *Aust. J. Chem.*, **35**, 2335 (1982). (e) P. Wormell and G.L.D. Ritchie, *J. Mol. Struct.*, **240**, 331 (1990). (f) J. Torbet, "Solution Behaviour of DNA Studied with Magnetically Induced Birefringence", in *Methods of Enzymology* (D.M.J. Lilley and J.E. Dahlberg editors), Vol. 211, 518 (Academic Press, San Diego, 1992).
56. (a) A.D. Buckingham, W.H. Prichard and D.H. Whiffen, *J. Chem. Soc. Chem. Commun.*, 51 (1965). (b) A.D. Buckingham, W.H. Prichard and D.H. Whiffen, *Trans. Faraday Soc.*, **63**, 1057 (1967). (c) M.P. Bogaard, A.D. Buckingham, M.G. Corfield, D.A. Dunmur and A.H. White, *Chem. Phys. Lett.*, **12**, 558 (1972). (d) P.B. Lukins and G.L.D. Ritchie, *J. Phys. Chem.*, **89**, 1312 (1985).
57. (a) T.G. Schmalz, C.L. Norris and W.H. Flygare, *J. Am. Chem. Soc.*, **95**, 7961 (1973). (b) T.M. Plantenga, H. Bultink, C. MacLean and J.A.B. Lohman, *Chem. Phys.*, **61**, 271 (1981). (c) P.R. Luyten, J. Bulthuis and C. MacLean, *Chem. Phys. Lett.*, **89**, 287 (1982).

CHAPTER 2 - PRINCIPLES AND OPERATION OF THE COTTON-MOUTON EFFECT APPARATUS

2.1 INTRODUCTION

This chapter briefly presents a discussion of the principles employed in the apparatus used to measure the temperature dependence of the Cotton-Mouton effect. A detailed analysis of the detection system, an appraisal of possible sources of error due to imperfections and misalignments of the optical components that comprise the apparatus, and the operation of the apparatus have previously been described,¹ and only the relevant aspects are outlined here.

Optical anisotropy is induced when a magnetic field is applied to a medium. The birefringence (anisotropy in the refractive index) is indirectly measured by conversion to a phase difference between the components of the electric vector of linearly polarized light parallel and perpendicular to the applied field. The emergent laser beam is elliptically polarized and the degree of ellipticity is characterized by a phase angle between the components, called the retardance, φ . This quantity is related to the birefringence by

$$\varphi = \frac{2\pi l}{\lambda}(n_{\parallel} - n_{\perp}) \quad (2.1)$$

where λ is the vacuum wavelength of light and l is the pathlength in the medium. Studies by Havelock² and others³ established the relationship

$$\varphi = 2\pi lCH^2 \quad (2.2)$$

where H is the magnetic field strength and C is a constant characteristic of the medium.

It is convenient to define the magnetic susceptibility and the magnetic hyperpolarizability in terms of the magnetic induction, B , which is related to H by the equation

$$B = \mu H \quad (2.3)$$

in which μ is the permeability of the medium. From an operational point of view, the definition of the molar Cotton-Mouton constant can be written, from equation (1.1), as

$${}_m C = \frac{\mu_0^2 \lambda}{27\pi} \int B_{\perp}^2 dl \left(\frac{\phi}{V_m^{-1}} \right) \quad (2.4)$$

in which V_m^{-1} , the reciprocal of molar volume, is proportional to the gas density. Gas densities were calculated from the measured pressures, p , and temperatures, T , using the virial expansion

$$p = \frac{RT}{V_m} (1 + BV_m^{-1}) \quad (2.5)$$

and tabulated density virial coefficients.⁴

In order to obtain the Cotton-Mouton first virial coefficient, A_C , from the pressure dependence of the Cotton-Mouton effect at a given temperature, the quantity

$${}_m C = \frac{2V_m \mu^2}{27} \left(\frac{n_{\parallel} - n_{\perp}}{B^2} \right)_{B=0} \quad (2.6)$$

was evaluated; this is related to the Cotton-Mouton virial coefficients by

$${}_mC = A_C + B_C V_m^{-1} \quad (2.7)$$

but, as explained elsewhere, the Cotton-Mouton second virial coefficient was not observable in the present studies.

It can thus be seen that to evaluate ${}_mC$ for a given sample of gas at a known temperature and density, it is necessary to determine the magnitude of the magnetic induction and to measure the retardance induced by that induction.

The apparatus used for measurements of the Cotton-Mouton effect in gases and vapours was originally designed and constructed in a previous study.¹ Subsequent to that study, various improvements have been made to the apparatus and the procedures have been revised, and these advances are described in this chapter. The apparatus was initially used at the University of Sydney and later at the University of New England.

2.2 PRINCIPLES OF THE COTTON-MOUTON EFFECT APPARATUS

In general, a convenient and sensitive technique of measuring the retardance is to apply a nulling birefringence, using some type of calibrated retarder. In this work, the difficulty of the small normalized transmitted intensity, I_ϕ , typically of the order of 10^{-11} , is circumvented by the application of modulation and the use of a lock-in analyzer to significantly enhance the signal-to-noise ratio.

As previously described,¹ the detection system used to measure the retardance is predicated on the attainable frequency of the applied magnetic field. Using the

present apparatus, the upper limit of the frequency of the magnetic induction is approximately 0.03 Hz, so that the optimal detection method will involve measuring the magnetic field-induced birefringence with a system time-constant of about 2 s. The detection system employed in previous studies¹ was found to be superior to the alternative method using Kerr cells, and was again used in the present studies. The induced retardance, ϕ , is converted to a rotation by a quarter-wave plate, modulated by a Faraday coil and continuously nulled by applying an equal and opposite rotation using a second Faraday coil; this technique is similar to the method used in a Kerr effect study.⁵ A schematic representation of the configuration of the apparatus is shown in Figure 2.1.

It is useful to describe the relationship between the experimental observables and the birefringence induced in the gas cell by a mathematical analysis of the detection system using the Mueller calculus.^{6,7} According to Stokes,⁶ a beam of light can be described by a Stokes vector $(I, M, C, S)^T$ in which the four parameters I , M , C , and S , represent the intensity, horizontal preference, $+45^\circ$ preference and right circular preference, respectively. Each optical component can be represented by a 4×4 real matrix whose elements are functions of the orientation and retardance of that component. In this scheme, the Cotton-Mouton cell is represented by the matrix for an ideal homogeneous linear retarder, where the azimuth of the fast axis is fixed. The quarter-wave plate is also treated as an ideal homogeneous linear retarder, with a relative retardance of $\pi/2$, whereas the analyzer is considered as an ideal homogeneous linear polarizer. Each Faraday coil is represented by the matrix for an ideal homogeneous circular retarder.

The general forms of the relevant matrices are as follows.^{6,8}

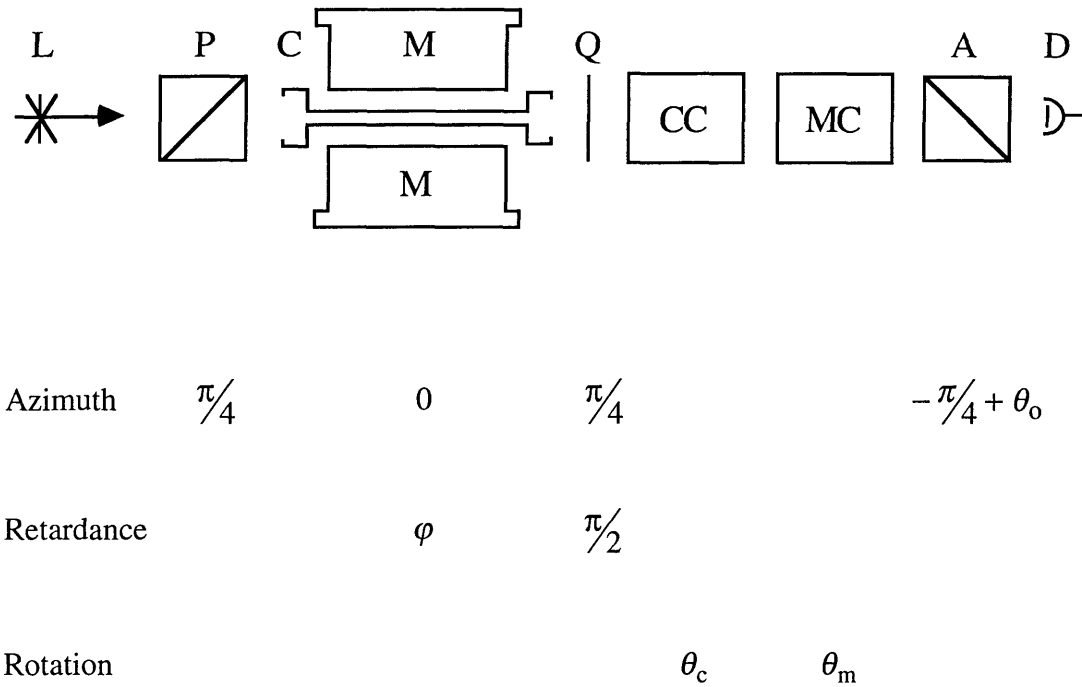


Figure 2.1 Optical configuration of the Cotton-Mouton effect apparatus

L, laser light source; P, polarizer; C, Cotton-Mouton gas cell; M, magnet; Q, quarter-wave plate; CC, compensating Faraday coil; MC, modulating Faraday coil; A, analyzer; D, detector.

- (a) The Mueller matrix for an ideal homogeneous linear polarizer is

$$\frac{1}{2} \begin{bmatrix} 1 & \cos 2\alpha & \sin 2\alpha & 0 \\ \cos 2\alpha & \cos^2 2\alpha & \cos 2\alpha \sin 2\alpha & 0 \\ \sin 2\alpha & \cos 2\alpha \sin 2\alpha & \sin^2 2\alpha & 0 \\ 0 & 0 & 0 & 0 \end{bmatrix}$$

in which α is the azimuth of the transmission axis.

- (b) The Mueller matrix for an ideal homogeneous linear retarder is

$$\begin{bmatrix} 1 & 0 & 0 & 0 \\ 0 & \cos^2 2\rho(1 - \cos \varphi) + \cos \varphi & \cos 2\rho \sin 2\rho(1 - \cos \varphi) & -\sin 2\rho \sin \varphi \\ 0 & \cos 2\rho \sin 2\rho(1 - \cos \varphi) & 1 - \cos^2 2\rho(1 - \cos \varphi) & \cos 2\rho \sin \varphi \\ 0 & \sin 2\rho \sin \varphi & -\cos 2\rho \sin \varphi & \cos \varphi \end{bmatrix}$$

in which ρ is the azimuth of the fast axis and φ is the relative retardance.

- (c) The Mueller matrix for an ideal homogeneous circular retarder is

$$\begin{bmatrix} 1 & 0 & 0 & 0 \\ 0 & \cos 2\theta & \mp \sin 2\theta & 0 \\ 0 & \pm \sin 2\theta & \cos 2\theta & 0 \\ 0 & 0 & 0 & 1 \end{bmatrix}$$

for a $\begin{cases} \text{left} \\ \text{right} \end{cases}$ circular retarder, in which θ is a Faraday rotation.

As the interest lies in detection of the intensity of the emergent beam in this configuration, only the first component of the final Stokes vector need to be evaluated.

The laboratory coordinate system is chosen so that the $+z$ axis is in the direction of propagation of the beam, the $+x$ axis is along the direction of polarization of the light beam emergent from the first polarizer, which is set at 45° to the magnetic field, and the $+y$ axis is orthogonal to x and z . The beam incident on the birefringent medium has a normalized Stokes vector of $(1,0,1,0)^T$.

Applying the Mueller calculus to the arrangement shown in Figure 2.1 and, assuming ideal conditions, the normalized intensity at the detector is found to be

$$2I = 1 - \cos(2\theta_m + 2\theta_c + \varphi + 2\theta_o) \quad (2.8)$$

where θ_m and θ_c are the rotations introduced by the modulator and compensator coils, respectively, and θ_o is an offset of the analyzer. The above equation can be simplified to

$$I = \sin^2\left(\theta_m + \theta_c + \frac{\varphi}{2} + \theta_o\right) \quad (2.9)$$

Taking θ_m such that

$$\left(\frac{\varphi}{2} + \theta_c + \theta_o\right) < \theta_m \leq 10^{-2} \text{ rad}$$

and invoking the small angle approximation, it can be shown that equation (2.9) reduces to

$$\begin{aligned} I &= \left(\frac{\varphi}{2} + \theta_c + \theta_o + \theta_m\right)^2 \\ &= \left(\frac{\varphi}{2} + \theta_c + \theta_o\right)^2 + 2\theta_m\left(\frac{\varphi}{2} + \theta_c + \theta_o\right) + \theta_m^2 \end{aligned} \quad (2.10)$$

If the modulating rotation is represented by $\theta_m^{(0)}\sin\omega t$, then the last term in equation (2.10) will give rise to a further d.c. term and a second harmonic term in $\cos 2\omega t$, hence

$$I = I_{\text{dc}} + I(\omega) + I(2\omega) \quad (2.11)$$

and it follows that the component of intensity modulated at the fundamental frequency, which can be selectively measured using a lock-in analyzer, is

$$I(\omega) = \theta_m(\varphi + 2\theta_c + 2\theta_o) \quad (2.12)$$

The detected intensity will therefore be zero, and this defines the “null condition”, when

$$\varphi = -2\theta_c - 2\theta_o \quad (2.13)$$

An offset, θ_o , introduced in the azimuth of the analyzer appears as a static rotation in equation (2.13) and, provided this offset is invariant during the time scale of a series of density-dependence measurements, it will not contribute to the error in the determination of φ .

The linear Faraday rotation of plane of polarization of a beam of light traversing a medium of length, l , and Verdet constant, V , in the presence of a longitudinal magnetic induction, B , can be described by the equation

$$\theta_F(B) = V l B \quad (2.14)$$

and as the magnetic induction is directly proportional to the Faraday coil current, i , then so is $\theta_F(B)$, thus the following relationship applies:

$$\theta_F(i) = ki \quad (2.15)$$

When the null condition, equation (2.13), is combined with the above equation, then

$$\varphi = -2\theta_c - 2\theta_o = -2k_c i \quad (2.16)$$

Therefore, if the calibration constant of the compensating Faraday coil, k_c , is known, then ${}_mC$, considered as A_C , can be determined from the measurement of the coil current, i , for the sample of gas under investigation.

2.3 INSTRUMENTATION

This section is concerned with a description of apparatus for the measurement of the Cotton-Mouton effect in gases and a discussion of the experimental procedure and data analysis. A schematic diagram of the apparatus is shown in Figure 2.2.

2.3.1 APPARATUS

The original apparatus was designed and constructed by Lukins,¹ and was subsequently used in this work. As it was of considerable interest to extend the studies to other molecules, many of which had smaller Cotton-Mouton effects than those previously examined, various modifications were introduced to extend the limit of resolution and to increase the ease of data acquisition.

Much of the equipment such as the framework, the magnet and its associated power supply, and optical components, was used without modification in these

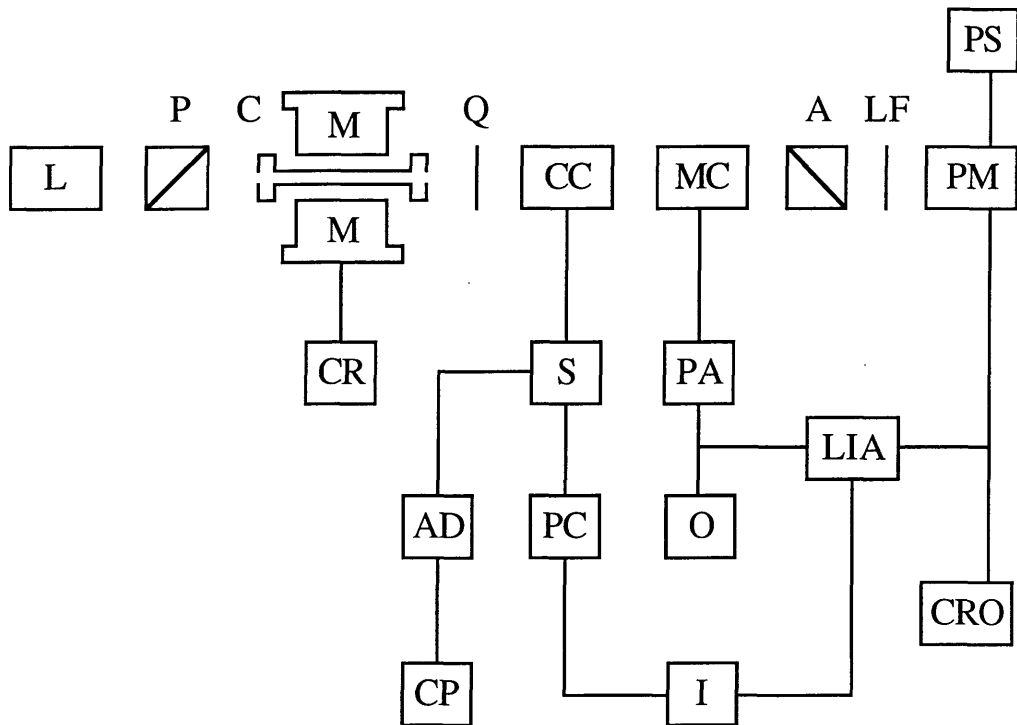


Figure 2.2 Apparatus for the measurement of the Cotton-Mouton effect in gases and vapours.

L, laser; P, polarizer; C, gas cell; M, magnet; Q, quarter-wave plate; CC, compensating coil; MC, modulating coil; A, analyzer; LF, laser line filter; PM, photomultiplier; PS, power supply; CR, current regulator; S, current sensing resistor and ammeter; PA, power amplifier; LIA, lock-in analyzer; AD, analog-to-digital converter; PC, programmable current regulator; O, oscillator; CRO, oscilloscope; CP, computer; I, integrator.

investigations. Field calibration measurements at ± 45 A were done periodically during the course of the project with a Bell 640 gaussmeter, Bell $\times 10^{1/4}$ % Hall probe and Fluke 8040A digital multimeter. The measured values of $\int B_{\perp}^2 dl$ agreed with the previously determined value of $3.289 \pm 0.045 \text{ T}^2\text{m}$. A helium-neon laser (Laser Electronics model LE202CP) rated at 2 mW at $\lambda = 632.8 \text{ nm}$ in the TEM₀₀ mode was used for all work described in this thesis. The polarizers were 13 mm aperture, schlieren-free calcite Glan-Taylor prisms which were rigidly set in their optical stands. Close tolerance, unmounted 19 mm mica quarter-wave plates were used for much of the work, although a mounted zero-order quarter-wave plate (Newport Model 05RP04), found to be superior in quality, that is, less noisy, was used in the latter studies. The procedure for the alignment of the optical components was as previously described.

The Cotton-Mouton cell was little changed in design from earlier work. To facilitate cleaning the inside of the brass cell body and replacement of electric heating tapes, Teflon ferrules were used, and the brass window mounts were modified so as to allow the cell to be removed without dismantling the large cage structure which supported the inner cell body and the end-windows.

A significant modification to the apparatus was the new design of the window and quarter-wave plate mounts. It was advantageous to minimise the Faraday rotation with the aim of obtaining more reliable data, particularly for those molecules with small Cotton-Mouton effects, and this necessitated the reduction of the magnetic flux through these components. The new mounts, of which the window mounts are shown in Plate 2.1, were made of steel and then heat treated to improve their magnetic shielding, thus significantly reducing the Faraday rotation compared to the previous arrangement. In addition, the new window mounts were of a novel design which minimised stress placed on each window, and made it easier to insert and rotate each

window to its best null position. Each window was housed in a bronze insert, and a Teflon spacer and Viton O-rings were used to secure the window within the steel mount, as shown in Figure 2.3. The mount for the quarter-wave plate was of similar design to that of the window mounts.

During the course of these studies, both Faraday coils used in this apparatus were replaced with new coils of similar design, because of the deterioration of the interior lacquer coating. For the new coils, the interiors were not coated with a lacquer; instead, all joints were sealed using a silicone-based cement. Distilled water passed through a 0.15 μm filter was again used as the core material. The coils were driven by power supplies described previously. Determination of the compensating coil calibration constant was repeated regularly using the Faraday coil procedure described by Lukins,¹ and the mean compensating coil calibration constant at $\lambda = 632.8$ nm was found to be

$$k = 0.6225 \pm 0.0021 \mu\text{rad mA}^{-1}$$

which is not dissimilar to the value of $k = 0.6263 \pm 0.0019 \mu\text{rad mA}^{-1}$ at $\lambda = 632.8$ nm obtained for the previous coil.

The photomultiplier tube and lock-in analyzer were employed as described by Lukins without alteration. After leaving the photomultiplier, the signal enters an Ithaco Dynatrac model 393 lock-in analyzer fitted with a filter to obtain the fundamental component at the modulation frequency. The amplifier and its power supply, used to drive the modulating coil, were also as previously employed.

In order to extend the sensitivity of the Cotton-Mouton effect apparatus, it was considered desirable to automate the data collection and handling phase of the

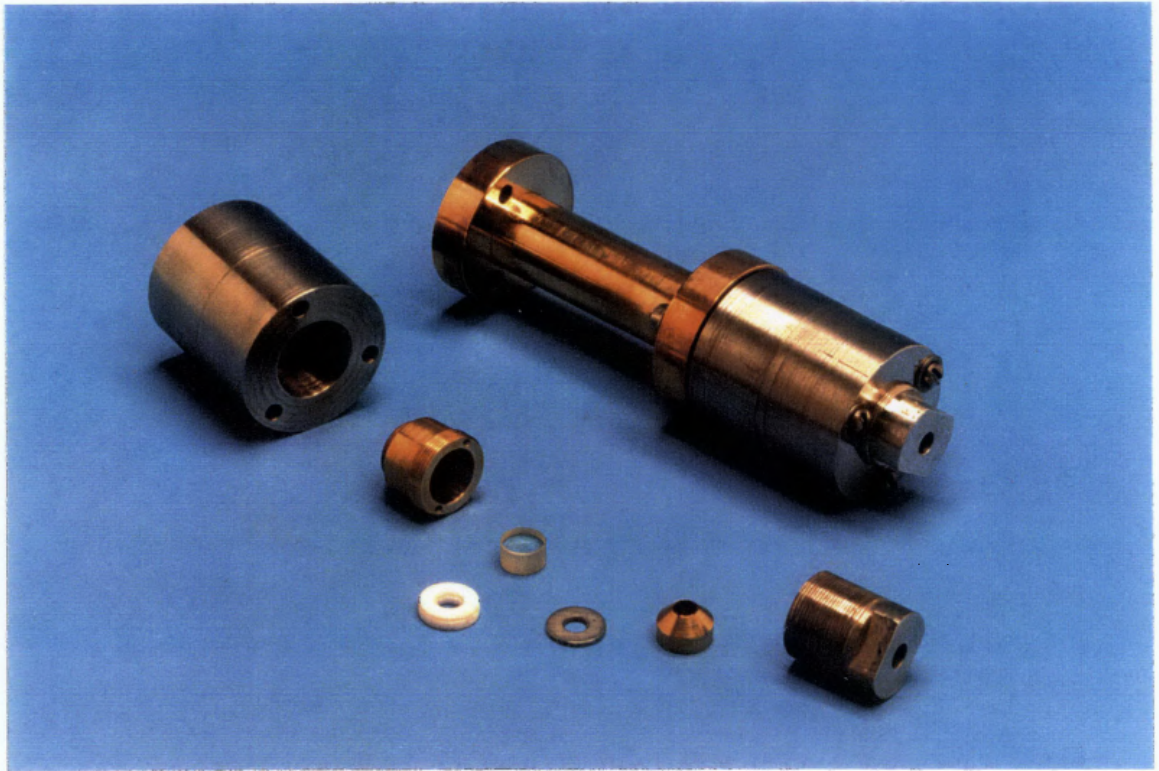


Plate 2.1 The window mounts.

One window mount is shown assembled and attached to a brass extension; the other mount is shown disassembled.

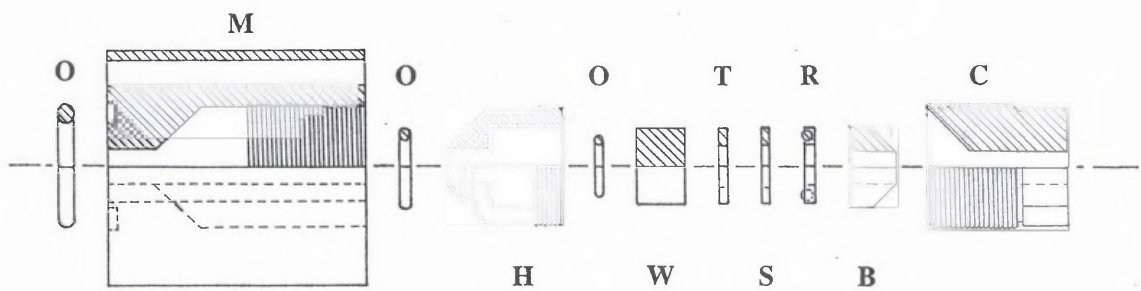


Figure 2.3 The window mount assembly (cross-sectional view partly shown).

O, Neoprene or Viton o-rings; M, heat-treated stainless steel window mount; H, brass housing for window; W, window; T, Teflon washer; S, stainless steel washer; R, stainless steel thrust race; B, brass insert; C, heat-treated stainless steel screw cap. Scale approximately 1 : 1.6.

procedure. The detection system was based on a continuous nulling facility provided by feedback from the lock-in analyzer to the compensator, using an integrator and a programmable attenuator to control the current entering the coil from the power amplifier. Therefore, the procedure involved plotting the lock-in analyzer output as a function of the current, referred to as the “nulling current”, through the compensating coil. The nulling current passing through the coil was determined by measuring the voltage, using a Fluke 8040A 4 $\frac{1}{2}$ -digit multimeter, across a 10 Ω resistor in series with the coil.

To enhance the capability of the detection system, the chart recorder was replaced by an Apple IIe microcomputer fitted with a Data Translation DT2832/5712 8-channel, 12-bit analog-to-digital converter, in conjunction with a DT710 screw terminal panel. The converter offers input ranges up to +10 V with an accuracy of $\pm 0.05\%$ of full scale range and nonlinearity ± 1 mV. A similar configuration with the Fluke multimeter was employed to monitor the input voltage. Time constants of the integrator (≈ 1 s) and the lock-in analyzer (125 ms at 3 mV sensitivity) were optimized to maintain stable operation of the feedback loop, with consideration given to rapid tracking with minimal overshoot. An offset in the azimuth of the analyzer was required for the feedback loop to operate, as the Kepco supply was unipolar. As no commercially available software was available for the task, two programs were written in Applesoft Basic to perform the following tasks shown below.

- (a) Data acquisition from the DT2832, followed by analysis and reporting. This program allows the user to vary the number of on/off cycles of the magnetic field for each sample. From the measurement of the nulling (or compensating coil) current, it is straightforward to obtain the retardance. Results are displayed graphically on the monitor, and averaged retardance

values printed on paper (Epson RX-80F/T printer). A typical graphic display is shown in Figure 2.4.

- (b) Calculation of ${}_mC$ values, given density virial coefficients for the gas under study and the measured temperature, pressure and calibration data. In addition, corrections for refractive index contributions were included.

With the incorporation of the computer interface, analysis of the performance of the detection system was straightforward and troubleshooting made much easier. Noise was manifested as a random fluctuation of the nulling current about its mean value. The peak-to-peak amplitude of this noise was typically 1×10^{-6} rad and, by averaging for 4 on/off cycles (≈ 8 mins), the standard deviation in the nulling current corresponded to about 5×10^{-7} rad. With longer averaging, often necessary for species with small Cotton-Mouton effects, the limit of resolution was estimated to be 2×10^{-7} rad. With possible systematic errors in calibrations, alignment, and measurement of the temperature and pressure, the errors in the values of ${}_mC$ obtained using this apparatus were estimated to be at most $\pm 3\%$.

The gas handling system underwent minor modifications to improve the ease of manipulating substances which were either gases at room temperature or liquids but essentially the same basic design and routine were employed in these studies. Throughout the present work, stainless steel piping, Swagelok and Cajon Ultra-Torr connectors, Nupro bellows and Whitey ball valves were replaced as appropriate. The system was periodically checked for leaks, and total leakage was determined to be less than 1 mmHg hr^{-1} . The pressure in the cell, or the pressure of gas in the manifold, was monitored by either a low pressure National Semiconductor LX1804GZ transducer, which was subsequently replaced by a Radio Shack 303-343 transducer (maximum pressure 200 kPa), or a Budenberg super test gauge (accuracy ± 1 kPa) at high pressures, as previously.

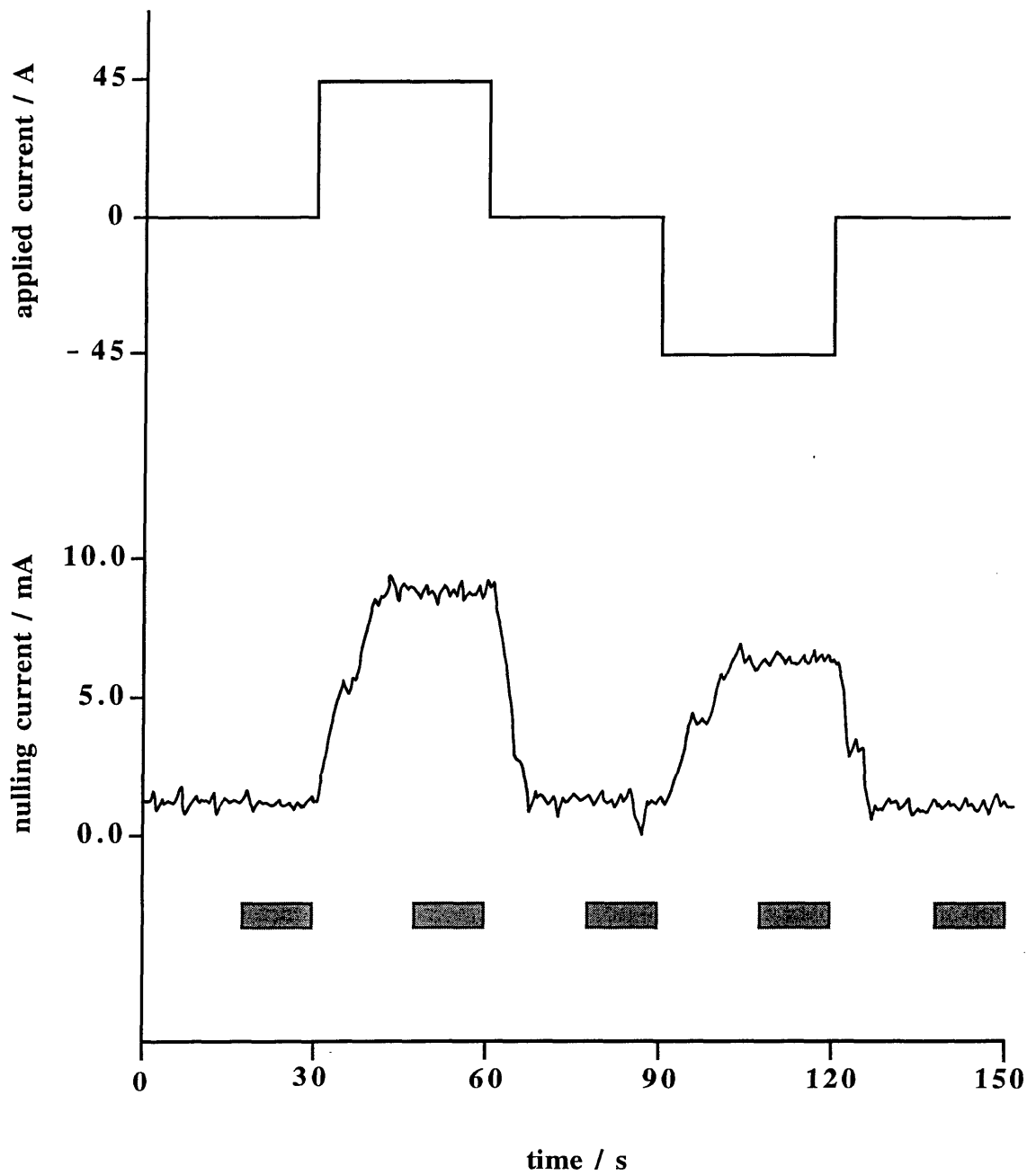


Figure 2.4 Simulated graph of waveforms for applied and nulling currents.

The nulling current shown corresponds to a retardance of $\sim 12 \mu\text{rad}$. Sampling periods are indicated by the shaded boxes.

A bath in which the Cotton-Mouton cell could be immersed was made using copper sheeting. The basic construction made it possible to undertake some measurements at below ambient temperatures and therefore to extend the temperature range further than was previously possible. Cooling mixtures used included ice-salt-water and dry ice-salt-water.

The temperature control and measurement system varied little from that used previously. To monitor the temperature of the cell during measurements, a close tolerance T-type thermocouple was positioned on the cell close to the end of one of the pole pieces. This thermocouple was used in conjunction with a Fluke model 2170A digital thermometer giving a resolution of 0.1°C, and this arrangement was also used to determine the temperature profile of the cell at each set temperature. Calibrations were performed at each set temperature by measuring the temperature every 1 cm along the entire length of the cell and the effective cell temperature taken as the average of these measurements. The temperature controller was generally not used, and Variac autotransformers, which proved to be more reliable, were preferred.

As cell window noise and drift are generally least under ambient temperature conditions, it is desirable to create smooth temperature gradients at the extremities of the cell. When operating at low temperatures, electric window mount heaters driven by variacs keep the windows near room temperature, thereby minimizing drift and avoiding condensation of atmospheric water vapour. These heaters may be operated at higher powers, elevating window temperatures to prevent condensation inside the cell when studying species of low volatility and to minimize bending of the laser beam as it passes through the cell due to spatial non-uniformities in gas density. As the cell windows are adversely affected at temperatures above 90°C, it was necessary to limit their temperature to $\approx 80^\circ\text{C}$ for high temperature studies, and this caused some difficulty due to beam-bending which was minimized by lowering the

maximum possible gas pressure for several species investigated in this work.

2.3.2 PROCEDURES

The alignment of the apparatus was periodically checked and adjusted when necessary; the procedure is described elsewhere.¹ During 1986, the entire apparatus was disassembled at the University of Sydney and reassembled at the University of New England. Subsequently, the apparatus was thoroughly tested and various studies of previously examined molecules were conducted and the results verified, prior to commencement of new work.

Various components were routinely checked, usually on a daily basis, before measurements were begun. Cell windows were cleaned, inserted and rotated to their best null position, one at a time. Particular care was taken during alignment of the cell windows to minimise Faraday rotation. Despite their excellent characteristics, the cell windows were normally the principal limitation to the performance of the apparatus. Any gross drift or window oscillation was eliminated by resetting or pressure cycling. Optical components were cleaned, and positioned precisely normal to the beam. Great care was taken to minimise scattering, reflections and air currents.

As noted elsewhere, a temperature dependence study is necessary to separate the hyperpolarizability and orientational terms. In addition, molecular interactions may contribute significantly to the observed magnetic birefringence, thus density dependence studies are required so as to obtain reliable values for the Cotton-Mouton constant appropriate to the free molecule. Experiments were therefore conducted over a range of temperature and, at each temperature, over a range of pressure. After the apparatus was aligned and its performance optimized, usually a painstaking and

arduous task, under the chosen experimental conditions, measurements were carried out at vacuum and at various pressures up to some chosen maximum pressure depending upon the magnitude of the effect, but not exceeding 75% of the equilibrium vapour pressure at the given temperature and any safety limitations. Particular care was taken to ensure that no inward leaks occurred when working at sub-atmospheric pressures due to the relatively large Cotton-Mouton effect of oxygen. At each pressure, including vacuum, about 4 cycles of ± 45 A peak amplitude square-wave current were applied to the magnet at the frequency of ≈ 0.03 Hz, and the nulling current recorded and analyzed to yield the field induced retardance. Each full density and temperature dependence study usually required two months, sometimes even longer, to complete.

All the substances investigated were subjected to gas chromatographic analyses and were found to have purities of $>99\%$ thus any uncertainties in the measurements due to impurities in the sample were considered to be negligible. For each sample, gas densities were calculated from the mean pressure and temperature using the virial equation and tabulated density virial coefficients. Hence values of ${}_mC$ were determined using a variation of equation (2.4)

$${}_mC = \frac{\mu_0^2 \lambda}{27\pi} \int B_{\perp}^2 dl \left(\frac{\partial \phi}{\partial \rho} \right)_{\rho=0} \quad (2.17)$$

Each value of ${}_mC$ was evaluated for each temperature at which measurements were taken and was assigned an error based on the standard deviation derived from the least squares analysis and an allowance for systematic errors described elsewhere.¹ Similar analyses were conducted for temperature dependences in which each ${}_mC$ value was weighted according to the error derived from density dependences, so that reliable values for the hyperpolarizability and orientational terms were obtained.

2.3 REFERENCES

1. P.B. Lukins, *Ph.D. Thesis* (University of Sydney, 1984).
2. T.H. Havelock, *Phys. Rev.*, **28**, 136 (1909).
3. (a) H.E. McComb, *Phys. Rev.*, **29**, 525 (1909). (b) C.A. Skinner, *Phys. Rev.*, **29**, 541 (1909). (c) G. Szivessy, *Handbuch der Physik*, **21**, 808 (1929). (d) J.W. Beams, *Rev. Mod. Phys.*, **4**, 133 (1932). (e) J.R. Partington, *An Advanced Treatise on Physical Chemistry*, **4**, 285 (Longmans, 1953).
4. J.H. Dymond and E.B. Smith, *The Virial Coefficients of Pure Gases and Mixtures* (Clarendon Press, Oxford, 1980).
5. A.D. Buckingham and H. Sutter, *J. Chem. Phys.*, **64**, 364 (1976).
6. W.A. Shurcliff, *Polarized Light: Production and Use* (Harvard University Press, Cambridge, Mass., 1962).
7. H. Mueller, *J. Opt. Soc. Am.*, **38**, 661 (1948).
8. E. Hecht and A. Zajac, *Optics* (Addison-Wesley, 1974).